Astron. Astrophys. 328, 203–210 (1997)

ASTRONOMY AND ASTROPHYSICS

SN Ia light curves and radioactive decay⋆

E. Cappellaro[1], P. A. Mazzali[2,3], S. Benetti[4], I.J. Danziger[3], M. Turatto[4,1], M. Della Valle[5], and F. Patat[5]

[1] Osservatorio Astronomico di Padova, vicolo dell'Osservatorio 5, I-35122 Padova, Italy
[2] National Astronomical Observatory, Mitaka, Tokyo 181, Japan
[3] Osservatorio Astronomico di Trieste, via G.B. Tiepolo 11, I-34131, Trieste, Italy
[4] European Southern Observatory, Alonso de Cordova 3107, Vitacura, Casilla 19001, Santiago 19, Chile
[5] Dipartimento di Astronomia, Università di Padova, vicolo dell'Osservatorio 5, I-35122 Padova, Italy

Received 10 June 1997 / Accepted 10 July 1997

Abstract. The absolute V light curves of 5 SNe Ia, selected to represent the known range of absolute luminosities at maximum for this class of objects, are presented. Comparison of the long term luminosity evolution shows that the differences seen at maximum persist, and actually increase with time, reinforcing the notion that intrinsic differences do exist among SNe Ia. Since such differences are not accounted for in the standard progenitor scenario, it becomes important to derive constraints for the models directly from the observations. In order to investigate the influence of the two most important parameters, that is the masses of the synthesized radioactive material and of the ejecta, a simple MC light curve model was used to simulate the luminosity evolution from the explosion to very late epochs ($\sim$ 1000 days). It was found that the observations require a range of a factor 10 in the masses of the radioactive material synthesized in the explosion ($M_{\rm Ni}$ = $0.1 - 1.1 {\rm M}_{\odot}$,) and a factor 2 in the total mass of the ejecta ($M_{\rm ej}$ = $0.7 - 1.4 {\rm M}_{\odot}$). Differences of a factor 2 in $M_{\rm Ni}$ seem to be present even among 'normal' SNe Ia.

Some evidence was also found that the deposition of the positrons from Co decay varies from object to object, and with time. In particular, the latest HST observations of SN 1992A seem to imply complete trapping of the positrons.

Key words: supernovae: general – supernovae: individual: SN 1991bg, SN 1991T, SN 1992A, SN 1993L, SN 1994D

1. Introduction

For many years type Ia supernovae (SNe Ia) were considered very reliable standard candles. However, more accurate CCD photometry for a rapidly growing number of SNe Ia has shown the existence of a range in the properties of this type of SNe. In particular, a correlation has been found between the absolute magnitude at maximum and the shape of the light curve (Hamuy et al., 1995; Riess et al., 1995). If this relationship can be well calibrated and other parameters are found to play a negligible role, the confidence in the use of SNe Ia as distance indicators may be restored.

A more subtle problem concerns the progenitors of SNe Ia. The standard scenario for SNe Ia is that a degenerate white dwarf in a binary system accretes matter from a close companion, either red giant or white dwarf (WD), until it reaches the Chandrasekhar mass ($M_{\rm Ch}$ = $1.4 {\rm M}_{\odot}$) and explodes, leaving no remnant (Nomoto et al., 1984; Woosley and Weaver, 1986). By tuning the relative masses and the separation of the stars in the binary system it is possible to obtain a very slow evolution and thus to explain the occurrence of SNe Ia among population II stars and hence in elliptical galaxies. If all SNe Ia events are triggered by the WD's mass reaching $M_{\rm Ch}$, independently of the initial conditions, it is natural to expect some homogeneity in the outcome of the explosions. One should nevertheless keep in mind the fact that type Ia supernovae occur in all types of galaxies. This theoretical view reinforced the empirical use of SNe Ia as standard candles. Lately, however, with the advent of larger samples, the observed diversity among SNe Ia appears to challenge that paradigm.

In particular, in the following we will show how the simple comparison of the late light curves of different SNe Ia requires the existence of a range in both the mass of radioactive material synthesized in the SN Ia explosions and the mass of the ejecta. Such differences can be seen not only in the well-known cases of peculiar SNe such as the bright SN 1991T and the faint SN 1991bg, but also within the group that has hitherto preserved the definition of 'normal' SN Ia.

2. Late light curves

We have compiled the absolute V light curves of five SNe Ia, namely SN 1991T, SN 1991bg, SN 1992A, SN 1993L and SN 1994D, combining unpublished observations with data from the literature.

In principle, bolometric light curves should be used for comparison with the models. Unfortunately, such data are available only for very few SNe, even in the best case they are lim-

⋆ Based on ESO observations collected at ESO-La Silla (Chile)

ited to the UVOIR spectral region and, with the exception of SN 1987A, they do not cover late epochs. However, both observations and spectrum synthesis indicate that in SNe Ia most of the deposited radioactive energy is re-radiated in the optical region and that, at phases later than 100d, the bolometric correction is constant and small, $m_{\rm bol-m_V} \leq 0.1 - 0.2$ mag (Suntzeff, 1996; Wheeler and Höflich, 1997). Therefore, in the following we simply assume that the bolometric correction for the V band is zero for all SNe Ia. Despite this crude approximation, this is not the major source of error, the uncertainties in the parent galaxies distance moduli and extinctions being in fact much larger.

The observations were retrieved from the archive of the ESO supernova monitoring programme (Turatto et al., 1990a), and are presented here for the first time, except for SN 1991bg, whose complete light curve has already been published in Turatto et al. (1996). These data have been supplemented, for the early phases, with published photometry from Phillips et al. (1992) for SN 1991T, Sunzeff et al. (1996) for SN 1992A, Filippenko et al. (1992) and Leibundgut et al. (1993) for SN 1991bg and Patat et al. (1996) for SN1994D.

Additionally, we included the photometry of SN 1992A obtained with WFPC2 on HST on Aug 2, 1994, 926 days after maximum. These observations, obtained in the framework of the SINS program (Kirshner et al. 1993) , consist of two sequences of four exposures through the F555W and the F439W filters, which are similar to the V and B bands, respectively. Exposure times for the individual frames were 900 sec for F555W and 1200 sec for F439W. The individual frames, calibrated in the standard pipeline, have been retrieved from the HST archive, properly aligned, and combined to eliminate cosmic rays. In the combined F555W image we found a stellar object whose offset from the field stars agrees to within 0.2 arcsec in both coordinates with the offset of SN 1992A as measured on the last ground-based observations (note that 1.2 arcsec west of the SN is a 23 mag background galaxy which appears as a stellar object on ground-based images). The SN magnitude, as measured by means of aperture photometry and calibrated relative to a sequence of local stars whose magnitudes were determined from the ground-based observations, is $V = 25.9 \pm 0.3$. The SN is not so evident in the combined F439W image which, however, is consistent with a $(B - V)$ colour close to 0.

The main data for the five SNe Ia are listed in Table 1, while the absolute V light curves are shown in Fig. 1. Absolute magnitudes were computed using the distance moduli given in the Tully (1988) catalog, except for SN 1993L, whose parent galaxy is not listed there. For this SN we use the distance given in the Leda extragalactic database[1]. Uncertainty in the absolute magnitudes arises mostly from the uncertainty concerning the distance scale. (both catalogs we are using adopt a Hubble constant of 75 km s^{-1} Mpc^{-1}). Although the errors in the absolute magnitudes may be quite large (of the order of ± 1 mag), the relative distances should be more reliable (typical errors are $\pm 0.2 - 0.3$ mag) and so the differences in magnitude between different SNe are expected to be real.

Magnitudes have been corrected for the total absorption A_V as estimated in the references indicated in Table 1.

The reference epochs for the light curves were chosen using the times of explosion estimated from spectrum synthesis and light curve modelling of the early photospheric phase. These range between 12 and 20 days prior to B maximum. The uncertainty in the determination of the time of maximum is negligible for our discussion, which is mostly concerned with the very late epochs.

In Table 1 we also list the quantities Δm_{15}^B, the difference in B magnitude from maximum to 15d, which is widely used to characterize the early light curve (col. 8), and Δm_{300}^V, the difference in V magnitude from maximum to 300d (col. 9). When observations at this epoch were not available, the value of Δm_{300}^V was derived by interpolation between the closest adjacent observations. Finally, we report the maximum expansion velocities of the Fe-nebula (col. 10). These are derived from models of the emission lines in spectra at epochs around 300d, except for SN 1991bg, whose spectral evolution was fast and for which a spectrum at 221d was used (Mazzali et al., 1997). The velocities tabulated correspond to the outer velocity of the Fe-nebula for which synthetic nebular spectra give a best fit to the late-time spectra of the SNe at hand (Mazzali et al., in preparation).

The SNe have been selected to represent the known range of luminosities of SNe Ia at maximum, going from the faint SN 1991bg to the 'average' SNe 1992A, 1993L and 1994D and the bright SN 1991T. The full range is about 2.3 mag at maximum. In particular, it appears that SN 1994D is consistently and significantly brighter than SNe 1992A and 1993L. This was also implied by Hamuy et al. (1995) on the basis of the different decline rates. Fig.1 shows that the differences in absolute magnitude persist to the very late phases, and actually increase with time, mostly reflecting the range in the early decline rates. Differences are about 3.5 mag already 2 weeks after maximum, and reach about 4 mag at 300d (Table 1), after which they apparently stop increasing.

The exception is SN 1991T, for which the luminosity after 500d stops declining. This results from an echo formed as the light emitted by the supernova near maximum light was reflected off dust in the CSM or ISM. (Schmidt et al., 1994; Danziger et al. unpublished spectra). Since there is no direct relation between the late-time luminosity of SN 1991T and the SN remnant itself, in the following we ignore the observations of SN 1991T at phases later that 500d.

From Table 1 the correlation between the absolute magnitudes at maximum and the early decline rate (Δm_{15}^B) is evident. In addition, it appears that at late phases brighter SNe have larger Fe-nebula expansion velocities (as already noticed by Danziger, 1994 and Turatto et al., 1996) and slower luminosity decline rates.

Another interesting feature shown in Fig. 1 is that, although the late light curves may appear quite linear on short time intervals, the decline rate actually slows down in the long run ($> 500d$). Unfortunately, the evidence is based on only one

[1] The Lyon-Meudon Extragalactic Database (LEDA) is supplied by the LEDA team at the CRAL-Observatoire de Lyon (France).

Table 1. SNe Ia data

SN	Gal	V_{max}	$(B-V)^*$	$M-m$	A_V	M_V	Δm_{15}^B	Δm_{300}^V	Neb.vel. [km s^{-1}]
1991bg	NGC4374	13.96	0.74	31.13	0.15[a]	−17.27	1.95[a]	8.4	2500
1993L	IC5270	13.2[#]	0.2	31.52	0.23[$]	−18.5[#]	1.5[#]	7.4	8000
1992A	NGC1380	12.54	0.00	31.14	0.00[b]	−18.60	1.47[d]	7.3	8500
1994D	NGC4526	11.90	−0.08	31.13	0.08[c]	−19.31	1.26[e]	7.3	9500
1991T	NGC4527	11.50	0.13	30.65	0.40[f]	−19.55	0.94[g]	6.7	10500

$*$ - measured at the epoch of the B maximum
$ - only galactic absorption included
# - the SN was discovered ten days after maximum. Its magnitude at maximum was extrapolated by comparison with SN 1992A.
Refs.: a - Turatto et al. (1996); b - Kirshner et al. (1993); c - Ho & Filippenko (1995); d - Hamuy et al (1996); e - Patat et al. (1996); f - Mazzali et al. (1995); g - Phillips (1993)

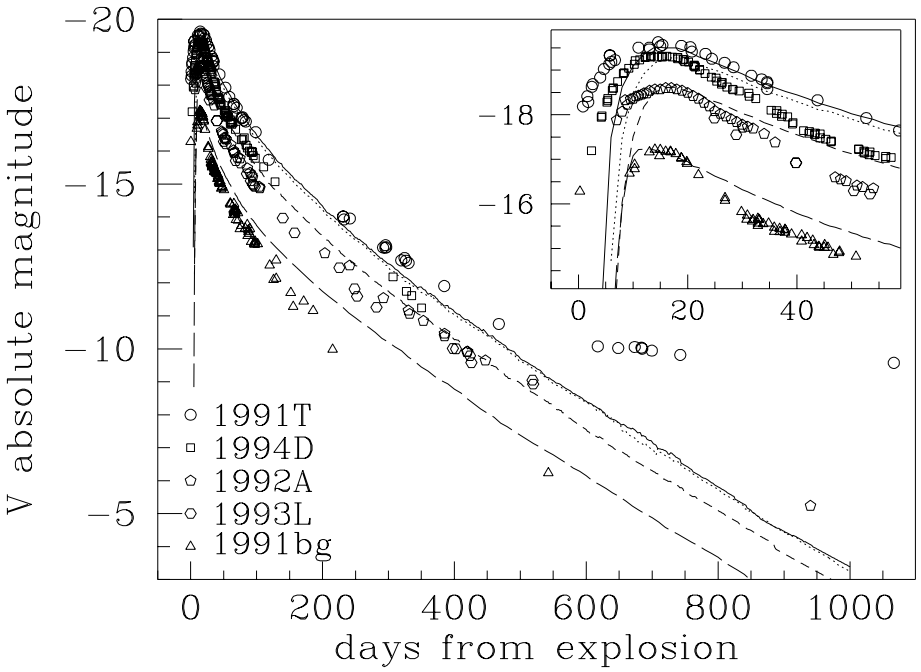

Fig. 1. The absolute V light curves of 5 SN Ia are compared with 4 models with different ejecta and Ni masses. The reference epochs is the time of explosion estimated from spectrum synthesis and light curve modelling of the early photospheric phase. From top to bottom the models are characterized by M_{ej} = 1.4, M_{Ni} = 1.1 (continuous line); 1.4, 0.8 (dotted); 1.0, 0.4 (short dashed) and 0.7, 0.1 (long dashed). For all models κ_e^+ = 7 is adopted. In the inset, the epoch near maximum is shown enlarged.

observation for each of the SNe 1991bg, 1992A and, possibly, 1993L. Since observations at such late epochs are difficult, and the photometry may be contaminated by phenomena not directly related to the remnant itself (eg. echoes in the case of SN 1991T or contaminating unresolved stars) this suggestion needs further confirmation. Meanwhile, it is worth exploring the implications of the effect if real.

3. Radioactive decay

Starting with the earliest attempts to model the SN light curves it has been clear that the fast expansion of the ejecta would result in a very rapid cooling and hence in a very rapid luminosity decline if only the thermal energy from the explosion had been available to power the SN.

On the contrary, for almost all types of SNe, the luminosity evolution is relatively slow. In particular, at epochs later than 150–200d the light curves decline almost linearly with rates in the range 0.8–1.5 mag/100d (Turatto et al., 1990b), implying the presence of a delayed energy input. The linear tail of the light curves corresponds to an exponential luminosity decline, suggesting that the radioactive decay of unstable heavy elements is a likely energy source, even though the decline rates for SNe Ia do not match the decay rates of known radioactive species.

Indeed, model calculations have shown that explosive silicon burning can produce unstable isotopes of iron group elements, in particular ^{56}Ni. ^{56}Ni decays into ^{56}Co, emitting γ-rays with an average energy per decay of 1.71 MeV (Burrows and The, 1990). Since the half-life of ^{56}Ni is relatively short ($\sim$ 6.1 days), this decay can only be important for the early light curve (the first 1–2 months).

^{56}Co is also unstable and decays into ^{56}Fe. The average energy available per decay is 3.67 MeV. Although most of this energy is released in the form of γ-rays, a significant fraction

of the ^{56}Co decays (19%) produces positrons. Positrons deposit their kinetic energy in the ejecta and then annihilate with electrons, producing two photons of energy $E_\gamma = m_e c^2$ each. The positron kinetic energy accounts for about 3.5% of the total ^{56}Co decay energy (Arnett, 1979; Axelrod, 1980). Because of its longer half-life (77.7 days), ^{56}Co decay can power the light curve of SNe for at least 2–3 years.

There is now ample evidence that the radioactive decay of ^{56}Ni and ^{56}Co provides most of the energy during the first 2-3 years, as was first suggested by Pankey (1962) and then, independently and more quantitatively, by Colgate and McKee (1969). The most convincing direct evidence has been the detection of γ-rays lines from ^{56}Co decay in the type II SN 1987A (Matz et al., 1988; Arnett et al., 1989; Palmer et al., 1993) and the temporal behaviour of the [CoII] lines at 10.52μ (Danziger et al., 1990) and 1.547μ (Varani et al., 1990). In the case of many SNe Ia, modelling of the late-time spectra indicates the presence of ^{56}Co lines whose intensity evolution is in agreement with the prediction from the ^{56}Co decay (Axelrod, 1980; Kuchner et al., 1994).

In the early phases of the SN evolution the density of the ejecta is still high enough that the γ-rays from radioactive decay are trapped in the ejecta and completely thermalized through Compton scattering with the free electrons. With the expansion the density decreases and the mean free path of the γ-rays increases. In the case of SNe II (and of at least a fraction of the SNe Ib/c) the mass of the ejecta is so large ($> 3M_\odot$) that even if their density decreases they remain optically thick to γ-rays for 2–3 years (Woosley, 1988). On the other hand, the ejecta become transparent to optical radiation a few months after maximum, and the observed decline of the optical luminosity reflects directly the decline of the radioactive energy supply. Indeed, the exponential tails of most SNe II light curves show the same e-folding time as that of the ^{56}Co energy release.

In the case of SNe Ia, the ejecta are less massive, while the Ni mass is larger ($M_{\rm Ni}/M_{\rm ej} \sim 0.5$ in SNe Ia vs. ~ 0.01 in SNe II). Also, there is evidence that in some cases Ni can be found in the outer layers. This allows an increasing fraction of the γ-rays to escape thermalization as time goes on, so that the light curves of SNe Ia decline more rapidly than the ^{56}Co energy release.

4. A simple light curve model

The observed differences in the light curves of SNe Ia may be attributed to many different factors. Accurate fitting of the light curve of a particular SN Ia may indeed require an ad-hoc explosion model and fine tuning of several parameters. However, this approach makes it difficult to disentangle the relative importance of the different parameters. Since we wanted to isolate the effects of the two arguably most interesting physical parameters, $M_{\rm Ni}$ and $M_{\rm ej}$, we developed a simple Monte Carlo code for the calculation of the bolometric light curve and did not use any particular explosion model. In particular, we made no effort to fit the shape of the light curve near maximum in detail.

Starting from a given density stratification and a distribution of Ni within the ejecta, the code computes the deposition of the γ-rays as a function of time with an MC scheme. The γ-ray energy sources are given by Sutherland & Wheeler (1984), while the opacity to γ-rays is assumed to be gray and to have a constant value $\kappa_\gamma = 0.027{\rm cm}^2\ {\rm g}^{-1}$, in agreement with recent calculations (Swartz et al., 1995). The energy released by the decay of ^{56}Co in the form of positrons (19% of the total) can only be transformed into γ-rays if the positrons annihilate.

The calculations show that with the expansion the ejecta become rapidly transparent to γ-rays. In particular, 200 days after the explosion the fraction of the γ-ray energy which is deposited in a typical model is only $\sim 0.5\%$. At this time the kinetic energy of the positrons may become the main contributor to the light curve, if a major fraction of it is deposited.

The early assumption was that positrons deposit all of their kinetic energy and annihilate almost on the spot (Axelrod, 1980). Subsequently, this idea has been questioned. For instance, Chan & Lingenfelter (1993) suggested that a significant fraction of the positrons manage to escape, possibly because of the presence of radially combed magnetic fields. On the other hand, Swartz et al (1995) argued that positrons cannot escape at all, otherwise a significant fraction of the radioactive decay energy would be lost.

Recently, it has been argued that to fit the late light curve of SNe Ia requires that the ejecta become progressively transparent also to positrons (Colgate et al., 1997), although with a longer time scale than for γ-rays (a typically adopted value is $\kappa_{e^+} = 7$ cm^2 g^{-1}). Describing the positron deposition by means of a positron opacity appears to be a natural approach, and we have adopted it in our light curve code. This gives us the freedom to manipulate the positron deposition as well as the transport of optical photons.

Our γ-ray source function for ^{56}Co therefore takes the form

$$S_{Co} = 0.81 s + 0.19 s D_{e^+} \quad (1)$$

where $s = 6.78\ 10^9[\exp(-t/\tau_{Co}) - \exp(-t/\tau_{Ni})]$ erg g^{-1} s^{-1} is the rate of energy production from the ^{56}Co decay (excluding the KE of the positrons), τ_{Co} and τ_{Ni} are the mean lifetimes of ^{56}Ni and ^{56}Co, respectively, and D_{e^+} is the positron deposition function. The positron KE accounts for an additional γ-ray source, which is given by

$$S_{e^+} = 0.036 s D_{e^+}. \quad (2)$$

When the γ-rays and the positrons deposit their energy, it is assumed that after thermalization this energy emerges as optical photons, so the contribution to PdV work is negligible. These optical photons can only contribute to the bolometric luminosity when they manage to escape from the ejecta. Given the high ejecta density, especially early-on, escape is not instantaneous. This is the reason why SNe Ia reach their L_{Bol} peak only 2–3 weeks after the explosion. The random walk of the optical photons in the expanding ejecta is also followed with an MC scheme. A gray optical opacity κ_{opt} is assumed where only a pure scattering opacity obtains. The ejecta are assumed to be

purely scattering. Time delay is accounted for by computing the time elapsed between successive scatterings, and updating the density before a new free flight is started. So finally for each optical energy packet we have a 'production time', corresponding to the time of emission, i.e. the time of deposition of the γ-ray packet from which the optical packet originates, and an 'emission time', the time when the packet eventually escapes from the ejecta. The difference between these two times becomes smaller and smaller as time goes on. The code allows us to reproduce not only the declining part of the light curve but also, at least roughly, the rising branch and the near-maximum phase. For 'average' SNe Ia we find that κ_{opt} = 0.15 cm^2 g^{-1} gives a reasonable fit to the rising branch and to the maximum of the light curve, whereas the late light curve is quite insensitive to the value of this parameter.

With these assumptions, the most important parameters for the light curve modelling are the mass of synthesized ^{56}Ni ($M_{\rm Ni}$), which determines the absolute luminosity, and the total mass of the ejecta ($M_{\rm ej}$), which determines the optical depth for the radiation from the radioactive decay. κ_{opt} affects mostly the time of maximum and its brightness, while κ_{e^+} influences the late-time behaviour. For larger κ_{opt} the maximum occurs later, and it is fainter and broader. For smaller κ_{e^+} the decay at late times is faster.

In the past, the consensus was that $M_{\rm Ni}$ and $M_{\rm ej}$ were exactly the same in all SNe Ia events, making them ideal standard candles. Estimates for $M_{\rm Ni}$ were in the range 0.5 to 0.7 M$_\odot$, while $M_{\rm ej}$ = $M_{\rm Ch}$. However, there is increasing evidence that both $M_{\rm Ni}$ and $M_{\rm ej}$ can be very different in different objects, although most SNe Ia appear to cluster around the historical values.

Since the SNe we have listed in Table 1 span a range of absolute magnitudes at maximum and of decline rates, it is quite likely that they cover a range of $M_{\rm Ni}$, and possibly also of $M_{\rm ej}$. To investigate this question further, we used our MC light curve code. As we discussed above, $M_{\rm Ni}$ and $M_{\rm ej}$ can be easily changed as input to the code. We took the approach of using a simple code and of not using any particular explosion model for any particular object, because literally hundreds of models, involving different $M_{\rm ej}$ and explosion mechanisms, and producing different amounts of ^{56}Ni, have now been produced by various groups, making it difficult to distinguish between them on the basis of their ability to fit observed light curves.

We adopted a W7 density structure, and rescaled it according to the epoch and to the values of $M_{\rm Ni}$ and $M_{\rm ej}$. We assumed that the Ni resides at the centre of the ejecta, in rough agreement with models of SN Ia explosions. The only exception is the model for SN 1991T. In this case, analysis of the early-time spectra suggests that there is an outer Ni shell (Mazzali et al. 1995).

Homologous expansion is assumed for rescaling to the appropriate epoch. Since different values of $M_{\rm Ni}$ and $M_{\rm ej}$ should lead to different kinetic energies of the ejecta, the $\rho(v)$ dependence is also rescaled. If we define the ratios X_{Ni} = $M_{\rm Ni}/0.60{\rm M}_\odot$ and X_{ej} = $M_{\rm ej}/M_{\rm Ch}$, we can rescale the kinetic energy per unit mass according to $KE \propto X_{Ni}/X_{ej}$.

In doing this we assume that all the KE is produced by burning to ^{56}Ni, neglecting the contribution of incomplete burning to intermediate mass elements (IME) such as Si. This is a reasonable approximation as long as $M_{IME}/M_{\rm Ni}$ is similar for all values of $M_{\rm Ni}$, which is of course not necessarily true. In particular, the energy will depend not just on $M_{\rm Ni}$, but also on a third parameter, the total mass of the newly synthesized elements. Indeed, in some cases, like SN 1991bg, the mass of these elements (e.g. Si-Ca, ^{54}Fe and ^{58}Ni) is comparable to, and probably greater than $M_{\rm Ni}$. Thus we expect our models to be an increasingly poor representation of the real properties of the SN the further $M_{\rm Ni}$ departs from the reference W7 value of 0.6M$_\odot$.

On the other hand, most SN Ia explosion models, including models for sub-Chandrasekhar explosions (Woosley & Weaver 1994), produce $\rho(v)$ functions whose shape is similar to that of W7, so in this respect our approximation should be reasonable. The velocity of a given shell in the ejecta is then rescaled according to $v/v_{W7} = (X_{Ni}/X_{ej})^{1/2}$, while the density of that shell is given by $\rho/\rho_{W7} = X_{ej}^{5/2} X_{Ni}^{-3/2}$.

Note that models with a ratio $M_{\rm Ni}/M_{\rm ej} \simeq 0.43$ have the same KE per unit mass as W7 (for which $M_{\rm Ni}/M_{\rm ej}$ = 0.60/1.38), and their density is simply the W7 density structure times X_{ej}, while models for which $X_{ej}^{5/2} = X_{Ni}^{3/2}$ have the same density as W7, but with each shell shifted to a velocity $v = v_{W7}(\frac{X_{Ni}}{X_{ej}})^{1/2}$. Since in the photospheric epoch the apparent photosphere forms at an almost constant value of the density, this may be a useful independent tool to investigate the values of $M_{\rm Ni}$ and $M_{\rm ej}$. This approach was adopted for all sub-Chandrasekhar models, but not for the SN 1991T ones, since the observed outer distribution of ^{56}Ni clearly must have a different effect on the kinetic energy. Thus, the KE for the SN 1991T model is probably underestimated.

Apart from the somewhat arbitrary rescaling of the velocity field, several other uncertainties must be kept in mind when comparing the model bolometric light curve with the observations:

1. Though we argued the V and bolometric light curves are not very different (cf. Sect. 2), they are not the same. A proper comparison would require a full NLTE light curve calculation, with the appropriate SN model. Such calculations do not exist as yet. Actually, even the bolometric light curve would require a more complex calculation than in our simple code. In particular, the opacities may change as a function of depth in the ejecta, and with time.
2. The SN may be clumpy, thus changing the deposition rate. This would also influence the nebular spectrum (Mazzali et al., in preparation).
3. The positon deposition is not well known. We discuss this point in the next section.
4. The steady-state assumption that the luminosity equals the instantaneous energy input breaks down after about 600 days, when the deposition time for the primary electrons produced by the γ-rays becomes long with respect to the dynamical and ionization time scales of the nebula (Axelrod, 1980). The ionization state may then be far from a steady state solution.

5. The distance and extinction to the various SNe are uncertain. By using a single source for the distances, we should at least minimize the relative errors, but the absolute numbers could change. For instance a Cepheid-based set of distances would require much bigger Ni masses.

5. Results

We selected the model parameters in order to fit the magnitude at maximum and the long-term decline rate of the individual SNe. Although less emphasis was given to the detailed fit of the light curves, we comment on the major discrepancies and the possible reasons.

In a first set of models we kept $\kappa_{e^+} = 7$ constant, and tried to obtain the best fit by varying $M_{\rm Ni}$ and $M_{\rm ej}$. In general, increasing $M_{\rm Ni}$ causes a shift of the light curve to brighter absolute magnitudes, while increasing $M_{\rm ej}$ delays the time of maximum and makes the decline of the light curve less steep.

The model fitting to the V light curves of the five SNe Ia is shown in Fig. 1. The models used for the fits are as follows.

For SN 1991bg, $M_{\rm ej}$ = 0.7M$_\odot$, $M_{\rm Ni}$ = 0.1M$_\odot$. This is in agreement with findings from modelling of both the photospheric and the nebular-epoch spectra (Mazzali et al. 1997), making SN 1991bg the best-studied case of a probable sub-Chandrasekhar mass SN Ia.

The V light curves of SNe 1992A and 1993L are practically indistinguishable once they have been corrected for extinction and relative distance. With the assumed distances, they reach a maximum of about -18.6 mag. The curves are fitted by a model with $M_{\rm ej}$ = 1.0M$_\odot$, $M_{\rm Ni}$ = 0.4M$_\odot$, which suggests they may also be sub-Chandrasekhar events. The model has the same $M_{\rm Ni}/M_{\rm ej}$ ratio as W7.

SN 1994D appears to be brighter than SNe 1992A and 1993L. The peak magnitude (-19.4) is well fitted by a model with $M_{\rm ej}$ = 1.4M$_\odot$, $M_{\rm Ni}$ = 0.8M$_\odot$, implying that the Ni production may be higher than in 'classical' SNe Ia. That SN1992A is fainter than average has also been demonstrated recently by Della Valle et al. (in preparation) who determined the distance to its parent galaxy using the method of the globular cluster luminosity function.

As can be seen from the insert of Fig. 1, a common feature of the models is that the rise to maximum is steeper and the early decline slower than observed. This could be improved by adopting different Ni distributions. In general, placing Ni further out than in the centre of the ejecta makes the light curve faster. We have computed a model using the W7 Ni distribution, which has a 'hole' in the central, highest density regions. This leads to faster escape of the optical photons after maximum, and produces a faster-declining light curve, which compares well with the observed ones. Still, W7 seems to be too faint to reproduce the light curve of SN 1994D and too bright for that of SN 1992A.

It should be noted here that the V light curves of SNe 1994D, 1992A and 1993L are very similar in shape. Thus, if the relative distances and extinctions were appropriately adjusted, all three SNe could be explained with a single explosion model.

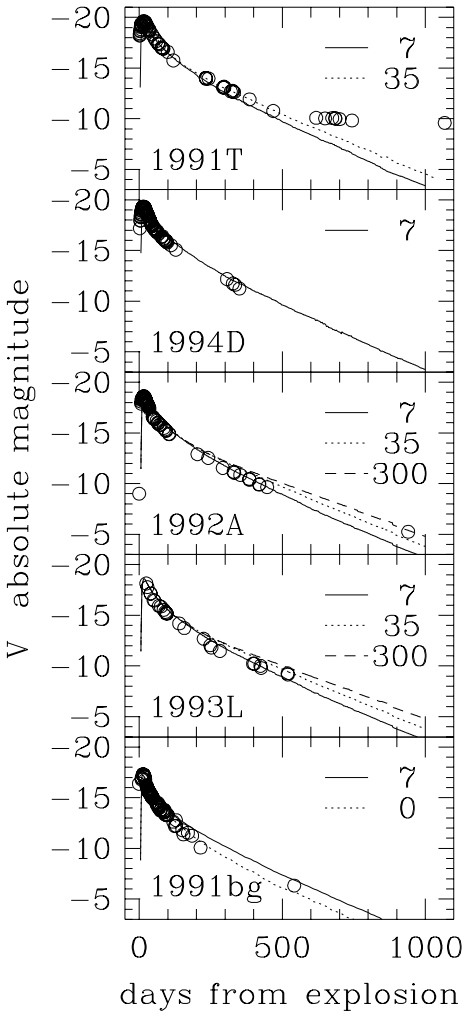

Fig. 2. Comparison of the V light curves of different SNe Ia with models for different values of the positron opacity, κ_e^+. The models for the individual SNe are characterized by different values of the radioactive Ni and ejecta masses. From top to bottom these are: 1991T: $M_{\rm ej}$ = 1.4M$_\odot$, $M_{\rm Ni}$ = 1.1M$_\odot$; 1994D: $M_{\rm ej}$ = 1.4M$_\odot$, $M_{\rm Ni}$ = 0.8M$_\odot$; 1992A and 1993L: $M_{\rm ej}$ = 1.0M$_\odot$, $M_{\rm Ni}$ = 0.4M$_\odot$; 1991bg: $M_{\rm ej}$ = 0.7M$_\odot$, $M_{\rm Ni}$ = 0.1M$_\odot$.

On the other hand, significant observational evidence also exists in favour of there being a difference between SNe 1994D and 1992A: SN 1994D is about 0.1 mag bluer at maximum, has a lower SiII line velocity near maximum (Patat et al. 1996, Fig.10a, where SNe 1994D, 1989B and 1990N appear to form one group and SNe 1992A and 1981B another), and broader nebular lines, with the SNe just mentioned falling again into two different groupings (Mazzali et al, in prep.). Thus, intrinsic differences between SNe generally labelled as 'classical' Ia are only beginning to receive the attention they deserve.

The last object we tried to fit is SN 1991T. For this SN, analyses of the early- (Mazzali et al. 1995) and late-time (Spyromilio et al. 1992) spectra suggest that the Ni mass is about 1M$_\odot$, and that a significant fraction of it is located in the high velocity outer part of the ejecta. If we assume $M_{\rm ej} = M_{\rm Ch}$, a

good fit can be obtained for $M_{\rm Ni}$ = 1.1M$_\odot$, of which 0.6M$_\odot$ is in the centre and 0.5M$_\odot$ is in the outer layers, which confirms previous findings.

Thus, it appears that a range of almost one order of magnitude in $M_{\rm Ni}$ is required to fit all the objects, and of at least a factor 2 in $M_{\rm ej}$. The range in $M_{\rm Ni}$ reflects the range in absolute magnitudes at maximum rather closely.

The models with κ_{e^+} = 7 fit the observations up to 400-500 days well for all the objects except 1991bg. In the case of SN 1991bg, starting 100–150 days after explosion the model is brighter than the observations. To reconcile the model with the observations, one could further decrease $M_{\rm ej}$, but this would lead to a very early maximum and would also cause problems for the interpretation of the spectra near maximum (Mazzali et al., 1997). Actually, a good fit to the late light curve of SN 1991bg can be obtained assuming that the opacity for positrons is much smaller than κ_{e^+} = 7. This is shown in the bottom panel of Fig. 2, where the model is calculated for the extreme case of complete transparency of the ejecta to positrons (κ_{e^+} = 0).

The opposite trend may be indicated by the SNe Ia 1993L and 1992A. At phases later than 400 days the observed light curves appear to decline at a rate slower than the prediction of the model with κ_{e^+} = 7. For SN 1994D, no observations are available at these very late epochs.

Finally, the light curve of SN 1991T is compatible with $\kappa_{e^+} > 7$. This may be real, but it may also indicate that the fraction of Ni on the outside is less than what we have assumed. Note, however, that if we distribute all the 1.1M$_\odot$ of Ni in the centre and compute a rescaled model with κ_{e^+} = 7, this has a larger KE than W7, and therefore a lower density, so it actually declines faster than the κ_{e^+} = 7 model shown in Fig.2. Another possibility is that $M_{\rm ej} > M_{\rm Ch}$. We computed a model with $M_{\rm ej}$ = 1.6M$_\odot$, $M_{\rm Ni}$ = 1.2M$_\odot$, which produces a light curve with a broad maximum and a slow decline. This model fits the observations reasonably well at all epochs, including the late phases. In the phase 60–150 days the model light curve is brighter than the observed one, but this is a feature common to all models shown in this paper. Even in this case, however, $\kappa_{e^+} > 7$ cannot be ruled out at 300–400 days. Clearly, SN 1991T deserves a much more detailed investigation than has been attempted here.

In principle we cannot exclude the possibility that, in addition to the radioactive decay, something else may contribute to the luminosity. In particular, given that spectra are not available at these very late epochs, we cannot entirely rule out contributions from echoes by circumstellar dust, as has been observed for SN 1991T. However, the luminosity decline of SN 1992A from 400 to 926 days (0.9 $\pm$ 0.1 mag/100d) is very close to the ^{56}Co decay rate (0.98 mag/100d,) and other energy sources do not seem to be required. As shown in Fig.2, this is the decline rate expected in the case of essentially complete trapping of the positrons (κ_{e^+} = 300) and complete transparency to the γ-rays.

6. Conclusions

The observed V light curves of different SNe Ia have been compared with models of the bolometric light curve obtained varying the values of $M_{\rm Ni}$ and $M_{\rm ej}$. The distribution of Ni was assumed to be central with the exception of the models for the bright SN 1991T, where an outer Ni shell was also used. The KE of the ejecta was rescaled according to $M_{\rm Ni}$ and $M_{\rm ej}$ in all cases except SN 1991T. Both $M_{\rm Ni}$ and $M_{\rm ej}$ influence the light curve, but while $M_{\rm Ni}$ influences mostly the level of the curve, $M_{\rm ej}$ affects also the time of maximum and the decline rate, so that a simultaneous fit to both the maximum and the late light curve, up to when the positrons begin to dominate, can only be obtained for a single set of $M_{\rm Ni}$ and $M_{\rm ej}$ values. Changes in the distribution of Ni and in the opacities between the various models would of course alter this result.

The comparison of the (late) light curves of SNe Ia with models confirms the suggestions derived from the analysis of observed spectra near maximum of the existence of a range in both the Ni and the ejecta mass.

It appears that objects which have usually been regarded as 'typical' SNe Ia may actually differ by more than 0.5 mag at maximum. This difference increases with time, suggesting that both $M_{\rm Ni}$ and $M_{\rm ej}$ may be significantly different in these objects (in particular, SN 1994D appears to be brighter and to have a larger $M_{\rm ej}$ than SNe 1992A and 1993L). Not surprisingly there appears to be a correlation between $M_{\rm Ni}$ and $M_{\rm ej}$ for the sample of 5 objects discussed here.

In general a reasonable fit to the late light curves can be obtained by assuming that the ejecta become progressively transparent also to the positrons generated in the Co decay. However, there are indications that the positron opacity is not constant from object to object or with time: the late light curve of SN 1991bg can be fitted if the assumption of complete transparency of the ejecta to the positrons is made, while those of SNe 1992A and 1993L after 500 days seem to require complete trapping of the positrons.

Acknowledgements. We are pleased to thank Ken Nomoto and Nikolai Chugai for useful discussions. P.A.M. acknowkedges receipt of a Foreign Research Fellowship at N.A.O., and is grateful to T. Kajino and the Dept. of Astronomy at the University of Tokyo for the hospitality.

References

Arnett, W. D.: 1979, ApJ 230, 37
Arnett, W. D., Bahcall, J. N., Kirshner, R. P., and Woosley, S. E.: 1989, ARA&A 24, 269
Axelrod, T. S.: 1980, Ph.D. thesis, UCRL 5294, Lawrence Livermore National Laboratory
Burrows, A. and The, L.-S.: 1990, ApJ 360, 626
Chan, K. W. and Lingenfelter, R. E.: 1993, ApJ 405, 614
Colgate, S. A., Fryer, C. L., and Hand, K. P.: 1997, in P. Ruiz-Lapuente, R. Canal, and J. Isern (eds.), Thermonuclear Supernovae, p. 273, Kluwer Academic Pub., Netherlands
Colgate, S. A. and McKee, C.: 1969, ApJ 157, 623
Danziger, I. J.: 1994, Mem. Soc. Astron. Ital. 65, 333
Danziger, I. J., Lucy, L. B., Bouchet, P., and Gouiffes, C.: 1990, in S. E. Woosley (ed.), Supernovae, p. 69, Springer-Verlag, New York

Filippenko, A.V. et al.: 1992, AJ 104, 1543
Hamuy, M., Phillips, M. M., Maza, J., Suntzeff, N. B., Schommer, R. A., and Avilés, R.: 1995, AJ 109, 1
Hamuy, M., Phillips, M. M., Suntzeff, N. B., Schommer, R. A., Maza, J., and Avilés, R.: 1996, AJ 112, 2391
Ho, L. C. and Filippenko, A. V.: 1995, ApJ 444, 165
Kirshner, R.P. et al.: 1993, ApJ 415, 589
Kuchner, M. J., Kirshner, R. P., Pinto, P. A., and Leibundgut, B.: 1994, ApJ 426, L89
Leibundgut B. et al.: 1993, AJ 105, 301
Matz, S. M., Share, G. H., Leising, M. D., Chupp, E. L., Vestrand, W. T., Purcell, W. R., Strickman, M. S., and Reppin, C.: 1988, Nat 331, 416
Mazzali, P. A., Chugai, N., Turatto, M., Lucy, L. B., Danziger, I. J., Cappellaro, E., Della Valle, M., and Benetti, S.: 1997, MNRAS 284, 151
Mazzali, P. A., Danziger, I. J., and Turatto, M.: 1995, A&A 297, 509
Nomoto, K., Thielemann, F.-K., and Yokoi, K.: 1984, ApJ 286, 644
Palmer, D. M., Schindler, S. M., Cook, W. R., Grunsfeld, J. M., Heindl, W. A., Prince, T. A., and Stone, E. C.: 1993, ApJ 412, 203
Pankey, T. J.: 1962, Ph.D. thesis, Howard University
Patat, F., Benetti, S., Cappellaro, E., Danziger, I. J., Della Valle, M., Mazzali, P. A., and Turatto, M.: 1996, MNRAS 278, 111
Phillips, M. M.: 1993, ApJ 413, L105
Phillips M.M. et al.: 1992, AJ 103, 1362
Riess, A. G., Press, W. H., and Kirshner, R. P.: 1995, ApJ 438, L17
Schmidt, B. P., Kirshner, R. P., Leibundgut, B., Wells, L. A., Porter, A. C., Ruiz-Lapuente, P., Challis, P., and Filippenko, A. V.: 1994, ApJ 434, L12
Spyromilio, J., Meikle, W. P. S., Allen, D. A., Graham, J. R., 1992, MNRAS 258, p. 53
Suntzeff, N. B.: 1996, in R. McCray and Z. Wang (eds.), Supernovae and Supernova Remnants, p. 41, Cambridge Univ. Press,Cambridge
Sutherland, P. G., Wheeler, J. C., 1984, ApJ 280, 282
Swartz, D. A., Sutherland, P. G., and Harkness, R. P.: 1995, ApJ 446, 766
Tully, R. B.: 1988, Nearby Galaxy Catalog, Cambridge University Press, Cambridge
Turatto, M., Benetti, S., Cappellaro, E., Danziger, I. J., Della Valle, M., Gouffies, C., Mazzali, P. A., and Patat, F.: 1996, MNRAS 278, 111
Turatto, M., Bouchet, P., Cappellaro, E., Danziger, I. J., Della Valle, M., Fransson, C., Gouffies, C., Lucy, L., Mazzali, P., and Phillips, M.: 1990a, Messenger 60, 15
Turatto, M., Cappellaro, E., Barbon, R., Della Valle, M., Ortolani, S., and Rosino, L.: 1990b, AJ 100, 771
Varani, G.-F., Meikle, W. P. S., Spyromilio, J., and Allen, D. A.: 1990, MNRAS 245, 570
Wheeler, J. C. and Höflich, P.: 1997, in R. Dufour and S. Torres-Peimbert (eds.), Proceedings of the Sixth Texas-Mexico Conference on Astrophysics, Astrophysical Plasmas, Revista Mexicana de Astronomia y Astrofisica, in press
Woosley, S. E.: 1988, ApJ 330, 218
Woosley, S. E. and Weaver, T.: 1986, ARA&A 24, 205
Woosley, S. E., Weaver, T., 1994, ApJ 423, 371

This article was processed by the author using Springer-Verlag LaTeX A&A style file *L-AA* version 3.